# Benchmark Quantum Monte Carlo calculations of the ground-state kinetic, interaction, and total energy of the three-dimensional electron gas

**I G Gurtubay[1,2], R Gaudoin[2] and J M Pitarke[1,3]**

[1] Materia Kondentsatuaren Fisika Saila, Zientzia eta Teknologia Fakultatea, Euskal Herriko Unibertsitatea, 644 Posta kutxatila, E-48080 Bilbo, Basque Country, Spain
[2]Donostia International Physics Center (DIPC), Manuel de Lardizabal Pasealekua, E-20018 Donostia, Basque Country, Spain
[3] CIC nanoGUNE Consolider and Centro de Física Materiales CSIC-UPV/EHU, Tolosa Hiribidea 76, E-20018 Donostia, Basque Country, Spain

E-mail: idoia.gurtubay@ehu.es

**Abstract.** We report variational and diffusion Quantum Monte Carlo ground-state energies of the three-dimensional electron gas using a model periodic Coulomb interaction and backflow corrections for N=54, 102, 178, and 226 electrons. We remove finite-size effects by extrapolation and we find lower energies than previously reported. Using the Hellman-Feynman operator sampling method introduced in Phys. Rev. Lett. **99**, 126406 (2007), we compute accurately, within the fixed-node approximation, the separate kinetic and interaction contributions to the total ground-state energy. The difference between the interaction energies obtained from the original Slater-determinant nodes and the backflow-displaced nodes is found to be considerably larger than the difference between the corresponding kinetic energies.

PACS numbers: 71.10.Ca, 71.15.-m

Submitted to: *JPCM*

## 1. INTRODUCTION

The homogeneous electron gas (HEG), which represents the simplest possible prototype of a many-fermion system, has been over the years a topic of intense research, as it often provides a good approximation for the description of valence electrons in simple metals and represents the basic ingredient for local and semilocal density-functional approximations.

One of the first exhaustive calculations of the ground-state energy of an interacting three-dimensional (3D) HEG was performed by Ceperley [1], using stochastic numerical methods. In this work, Ceperley used variational Monte Carlo (VMC) to obtain an upper bound to the ground-state energy. More accurate ground-state energies can be computed by using the more sophisticated diffusion Monte Carlo (DMC) approach, which projects out the true ground state of the system from a trial wave function [2]. However, this method yields a bosonic ground state even for a fermionic system which needs to have an antisymmetric ground state. In order to overcome this problem, the fixed-node (FN) approximation [3] has been applied; this approximation constrains the nodes of the ground-state wave function to those of a trial wave function. In spite of this constraint, the FN method has proven to be useful for the calculation of the ground-state energy and other electronic properties for atoms [4, 5], molecules [6, 7], solids [8, 9] and the two-dimensional (2D) electron gas [10, 11, 12]. As an alternative to overcome the sign-problem for fermions, Ceperley and Alder [13] developed the so-called released-node DMC, which has the limitation that statistical fluctuations grow very rapidly and statistical noise can dominate the signal even before converging to the ground state. The size of the system that can be simulated is also limited in this method. Nonetheless, these released-node data have been widely used in the framework of density-functional calculations.

With the improvement of computing capabilities and algorithms, new calculations have been attempted in order to improve the Ceperley-Alder DMC data. Ortiz and Ballone [14] extended these calculations to larger system sizes and polarized systems. Kwon *et al.* [15] introduced backflow and three-body correlations in the wave function, showing an improvement in the FN result beyond that given by Slater-Jastrow wave functions for a given finite system (see also [16], [17] and [18]). Both Ortiz and Ballone [14] and Kwon *et al.* [15] studied the size dependence and extrapolated their results to the thermodynamic limit; however, they assumed that the size dependence for VMC and DMC is the same, and they used VMC data to extrapolate the corresponding DMC calculations.

Fixed-node DMC is known to yield the exact ground-state energy of a many-electron system for a given nodal structure. Nevertheless, the DMC expectation value of any operator that does not commute with the Hamiltonian differs from the exact value, the error being linear in the difference between the trial and the projected wave function. Recently, an effective method based on the Hellman-Feynman (HF) theorem was devised to calculate the exact expectation value of such an operator [19] as, for example, the

interaction energy.

In this paper, we use the HF sampling introduced in [19] to report benchmark DMC calculations of the two (kinetic and interaction) separate contributions to the ground-state energy of a paramagnetic 3D electron gas with $r_s = 2$.‡ We include backflow correlation effects and we demonstrate that previously extrapolated results are artificially lowered by assuming that the VMC and DMC size dependences coincide. However, we find that DMC size dependences are similar with or without backflow correlation effects. The use of the HF sampling allows to compute the exact (within the fixed node approximation) interaction energy in the framework of the modified periodic Coulomb (MPC) scheme, and we show that this interaction energy can also be obtained from the integration of the spherically averaged wave-vector dependent diagonal structure factor [20]. Furthermore, we find that the HF-sampling scheme works efficiently even for very large systems.

Hartree atomic units (a.u.) are used throughout, i.e., $\hbar = |e| = m_e = 4\pi\epsilon_0$=1. The atomic unit of energy is $e^2/a_0 = 27.2$ eV, $a_0$ being the Bohr radius. All the calculations presented in this work have been performed by using the CASINO code [21].

## 2. QUANTUM MONTE CARLO

In VMC the ground-state energy, $E_{VMC}$, is estimated as the expectation value of the Hamiltonian with an approximate trial wave function, $\Psi_T$: $E_{VMC} = \langle\hat{H}\rangle_{VMC} = \langle\Psi_T|\hat{H}|\Psi_T\rangle/\langle\Psi_T|\Psi_T\rangle$. The integrals are evaluated by importance-sampled Monte Carlo integration. The trial wave function contains parameters, whose values are obtained from an optimization procedure formulated within VMC. There are no restrictions on the form of the trial wave function, and VMC does not suffer from a fermion sign problem. However, the choice of the approximate trial wave function is very important, as it directly determines the accuracy of the calculation. We have used VMC methods mainly to optimize the parameters involved in the trial wave functions by variance and energy minimization; our most accurate calculations, however, have been performed within DMC.

In DMC the ground-state component of a trial wave function is projected out by evolving an ensemble of electronic configurations using the imaginary-time Schrödinger equation. The fermionic symmetry is maintained by the fixed-node approximation [3], in which the nodal surface of the DMC wave function is constrained to equal that of the trial wave function. The fixed-node DMC energy, $E_{FN} = \langle\hat{H}\rangle_{FN} = \langle\Psi_0^{FN}|\hat{H}|\Psi_0^{FN}\rangle/\langle\Psi_0^{FN}|\Psi_0^{FN}\rangle$, is higher than the exact ground-state energy $\langle\hat{H}\rangle = \langle\Psi_0|\hat{H}|\Psi_0\rangle/\langle\Psi_0|\Psi_0\rangle$, and they become equal only when the fixed nodal surface is that of the exact ground state, $\Psi_0$. Apart from the fixed-node error, DMC yields the true ground-state energy independently of the form chosen for the trial wave function. The fixed-node error can be reduced by optimizing the nodal surfaces of the

‡ $r_s$ is the dimensionless parameter $r_s = a/a_0$ where $a_0$ is the Bohr radius and $a$ is the radius of a sphere that encloses one electron on average.

trial wave function.

### *2.1. The Slater-Jastrow backflow trial wave function*

The standard Slater-Jastrow (SJ) wave function can be written as

$$\Psi_{\rm SJ}(\mathbf{R}) = e^{J(\mathbf{R})}\Psi_{\rm S}(\mathbf{R}), \tag{1}$$

where $\mathbf{R}$ is a $3N$-dimensional vector denoting the position $\mathbf{r}_i$ of each electron. The nodes of $\Psi_{\rm SJ}(\mathbf{R})$ are defined by the Slater part of the wave function, $\Psi_{\rm S}(\mathbf{R})$, which takes the form $\Psi_{\rm S} = D_\uparrow D_\downarrow$, $D_\sigma$ being a Slater determinant of single-particle orbitals of spin $\sigma$. In the case of a HEG, these orbitals are Hartree-Fock solutions for the finite periodically repeated electron gas, which are simply plane waves. The number of electrons $N$ has been chosen such that the ground state is a closed shell configuration, so the wave function can be chosen to be real and there is no degeneracy. The Jastrow correlation factor, $e^{J(\mathbf{R})}$, contains an electron-electron and a plane-wave term, as described in [22]. We did not include a symmetric three-electron Jastrow term.§ The Jastrow factor, being a positive definite function, keeps electrons away from each other and greatly improves wave functions in general, but it does not modify the nodal surface of the wave function.

One way of reducing the FN error is to alter the nodes of the wave function by introducing backflow correlations [16], thus replacing the coordinates $\mathbf{R}$ in the Slater part of the wave function by the collective coordinates $\mathbf{X}$. The Slater-Jastrow backflow (SJB) trial wave function reads

$$\Psi_{\rm SJB}(\mathbf{R}) = e^{J(\mathbf{R})}\Psi_{\rm S}(\mathbf{X}). \tag{2}$$

The new coordinates for each electron are given by

$$\mathbf{x}_i = \mathbf{r}_i + \xi_i(\mathbf{R}), \tag{3}$$

$\xi_i$ being the backflow displacement of particle $i$, which depends on the position of every electron in the system. Details of the specific form of the backflow function used for the HEG can be found in [16].

### *2.2. Hellman-Feynman sampling*

Given an arbitrary operator $\hat{O}$, the fixed-node DMC method yields by construction the normalized expectation value $\langle\hat{O}\rangle_{FN\text{–}DMC} = \langle\Psi_T|\hat{O}|\Psi_0^{FN}\rangle/\langle\Psi_T|\Psi_0^{FN}\rangle$, which is not the true FN ground-state expectation value $\langle\hat{O}\rangle_{FN} = \langle\Psi_0^{FN}|\hat{O}|\Psi_0^{FN}\rangle/\langle\Psi_0^{FN}|\Psi_0^{FN}\rangle$, unless the operator $\hat{O}$ commutes with the Hamiltonian, the leading term of this error being linear in the difference between $\Psi_T$ and $\Psi_0^{FN}$. In conjuntion with VMC, this error can be reduced by one order by using the so-called extrapolated estimator, $2\langle\hat{O}\rangle_{FN\text{–}DMC} - \langle\hat{O}\rangle_{VMC}$. In practice, extrapolated estimators work well when the trial wave function is very close to the ground state, but they can be untrustworthy when the trial wave function is poor. A

§ We found that for the density considered in this work, the effect of the three-body term was not statistically significant in conjunction with backflow, which gives the best energy. This is in agreement with [16].

correct sampling for these operators can be achieved by using future walking [23, 24] or reptation Monte-Carlo [25]; however, these methods aim at sampling $\Psi_0^{FN}\Psi_0^{FN}$ instead of the regular DMC distribution [2], $\Psi_T\Psi_0^{FN}$, so they are not straightforward additions to the DMC algorithm.

An alternative to achieve a correct sampling of operators (diagonal in real space) that do not commute with the Hamiltonian has been reported recently [19]. The advantage of this so-called HF sampling is that it samples the usual DMC distribution, $\Psi_T\Psi_0^{FN}$, and it is, therefore, straightforward to implement on a DMC algorithm. We give here a sketch of the method; a detailed derivation can be found in [19]. Given a Hamiltonian of the form $\hat{H}(\alpha) = \hat{H} + \alpha\hat{O}$ and the associated fixed-node ground-state energy $E_{FN}(\alpha) = \langle\hat{H}(\alpha)\rangle_{FN}$, first-order perturbation theory for $\Psi_0^{FN}$ yields a fixed-node equivalent of the HF theorem‖

$$\langle\hat{O}\rangle_{FN} = \frac{\partial E_{FN}(\alpha)}{\partial\alpha}\Big|_{\alpha=0}. \tag{4}$$

Direct application of the HF derivative to the regular DMC algorithm at timestep $i$ gives:

$$O_i^E = \frac{\partial E_i(\alpha)}{\partial\alpha}\Big|_{\alpha=0} = \overline{O_i^L} - t\left(\overline{E_i^L X_i} - \overline{E_i^L}\cdot\overline{X_i}\right), \tag{5}$$

$t$ is an auxiliary parameter and $\overline{O_i^L}$ is the standard DMC estimator at time step $i$:

$$\overline{O_i^L} = \sum_j^{N_w} \omega_{i,j}\; O_{i,j}^L, \tag{6}$$

where $\omega_{i,j}$ is the total weight of walker $j$, and $O_{i,j}^L = \hat{O}\Psi_T/\Psi_T$ with the trial wave function, $\Psi_T$, evaluated for walker $j$ at time step $i$. $\overline{X_i}$ is the DMC estimator at time step $i$ of a new variable per operator $X_{i,j} = \frac{1}{i}\sum_{k=1}^{i} O_{k,j}^L$. The fixed-node DMC estimate, which we call $\langle\hat{O}\rangle_{FN\text{–}DMC}$, is obtained averaging Equation (6) over all $i$.

The correction term, $\Delta O_i^E = -t\left(\overline{E_i^L X_i} - \overline{E_i^L}\cdot\overline{X_i}\right)$, involves information which can be directly obtained from the DMC algorithm, such as the local energy, $E_{i,j}^L = \hat{H}\Psi_T/\Psi_T$, and the new variable, $\overline{X_i}$, which involves no more than an extra summation step during the sampling. The true FN estimate, which we call $\langle\hat{O}\rangle_{HF}$, is obtained averaging $O_i^E$ over all $i$.

Exponentially limiting the depth of the history in $X_{i,j}$ allows one to considerably improve sampling and reduce statistical noise without reintroducing a significant bias [27].

## 3. Details of the calculations

We have studied an unpolarized 3D HEG consisting of 54, 102, 178, and 226 electrons in a face-centered-cubic simulation cell subject to periodic boundary conditions.

‖ The Hellman-Feynman theorem has also been applied previously in QMC for deriving accurate expectation values of observables [26].

The parameters in the SJB trial wave functions were obtained by first minimizing the variance of the local energy [28, 29] and then minimizing the energy [30]. The specific forms of the Jastrow and backflow functions are described in [22] and [16]. The 2-body Jastrow term ($U$) and backflow ($\eta$) terms consist on power expansions in the electron-electron distance with expansion orders $N_U$=$N_\eta$=8 and the parameters were allowed to depend on the spin parameters of the electron pairs. The cutoff lengths at which both $U$ and $\eta$ go smoothly to zero, $L_U$ and $L_\eta$, were optimized, but they adjusted themselves to the maximum allowed values, i.e., the Wigner-Seitz radius. The plane-wave term in the Jastrow factor included 128 reciprocal-lattice vectors of the simulation cell. We used a sufficiently small time step (0.003 a.u.), to avoid finite-time-step errors, and a target population of 800 configurations in all our DMC calculations, making population-control bias negligible.

Because our QMC calculations are performed using a finite simulation cell subject to periodic boundary conditions,¶ the energy per particle is calculated at several system sizes and then the results are extrapolated to infinite system size. Finite-size effects in the kinetic energy are typically taken into account by noting that they are roughly proportional to the corresponding finite-size errors in the Hartree-Fock kinetic energy. Coulomb finite-size effects in the interaction energy of a HEG, which arise from the spurious interaction between an electron and the periodically repeated copies of its exchange-correlation (xc) hole, can be reduced either by adding the correction proposed by Chiesa *et al.* [33] to the usual Ewald energy or by using the MPC [31, 34, 35, 36] interaction. In this work, Coulomb finite-size effects were reduced by using the MPC scheme, where the Hartree energy is calculated with the Ewald interaction while the xc energy is calculated using $1/r$ within the minimum image convention, that is, reducing the interelectron distance into the Wigner-Seitz cell of the simulation cell. The MPC interaction was used for the branching factors and for computing energies in DMC. According to Drummond et al. [31] the Ewald interaction distorts less the xc hole when calculating branching factors in DMC. However MPC branching is faster and so potentially allows bigger systems. The trade-off is therefore between better convergence due to the xc hole being more accurate, or due to being able to go to bigger systems quicker. We have chosen the latter.

## 4. Results and discussion

### *4.1. Ground-state total energy*

VMC and DMC ground-state total energies of a HEG of $r_s = 2$ for $N$=54, 102, 178, and 226 electrons, as obtained by using either SJ or SJB trial wave functions within the MPC scheme, are given in table 1. These energies are also displayed by open symbols

¶ We used the Gamma point only. The recent analysis of Drummond *et al.* [31] showed that the Γ-point extrapolated SJ-DMC energies of a HEG agree within error bars with the results obtained by using the more sophisticated twist-averaged boundary conditions [32].

in figure 1 with their corresponding error bars, which are less than 20% of the symbol size. Both VMC and DMC ground-state energies show the usual finite-size effects. For comparison, table 1 also displays the DMC-SJ energies obtained by using the Ewald interaction.

**Table 1.** VMC and DMC ground-state total energies, $E_{VMC}$ and $E_{DMC}$, as obtained with the use of SJ and SJB trial wave functions for a HEG of $r_s$=2 for $N$= 54, 102, 178, and 226 electrons and the MPC interaction. The column denoted with Ewald shows the DMC energies for the SJ wave function and the Ewald interaction. The entry $N = \infty$ corresponds to the extrapolated values obtained from Equation (7).

| | SJ wave function | | | SJB wave function | |
|---|---|---|---|---|---|
| | MPC | | Ewald | MPC | |
| $N$ | $E_{VMC}$ (Ha/e) | $E_{DMC}$ (Ha/e) | $E_{DMC}$ (Ha/e) | $E_{VMC}$ (Ha/e) | $E_{DMC}$ (Ha/e) |
| 54 | 0.00847(2) | 0.00693(4) | 0.00426(2) | 0.00656(2) | 0.00579(2) |
| 102 | 0.00328(1) | 0.00202(2) | 0.00081(2) | 0.001398(8) | 0.00077(2) |
| 178 | 0.01057(1) | 0.00950(2) | 0.00892(2) | 0.008510(8) | 0.00801(1) |
| 226 | 0.003490(8) | 0.00246(2) | 0.00202(2) | 0.001710(5) | 0.00123(1) |
| $\infty$ | 0.003886(5) | 0.00301(1) | 0.00331(3) | 0.002021(4) | 0.001621(7) |

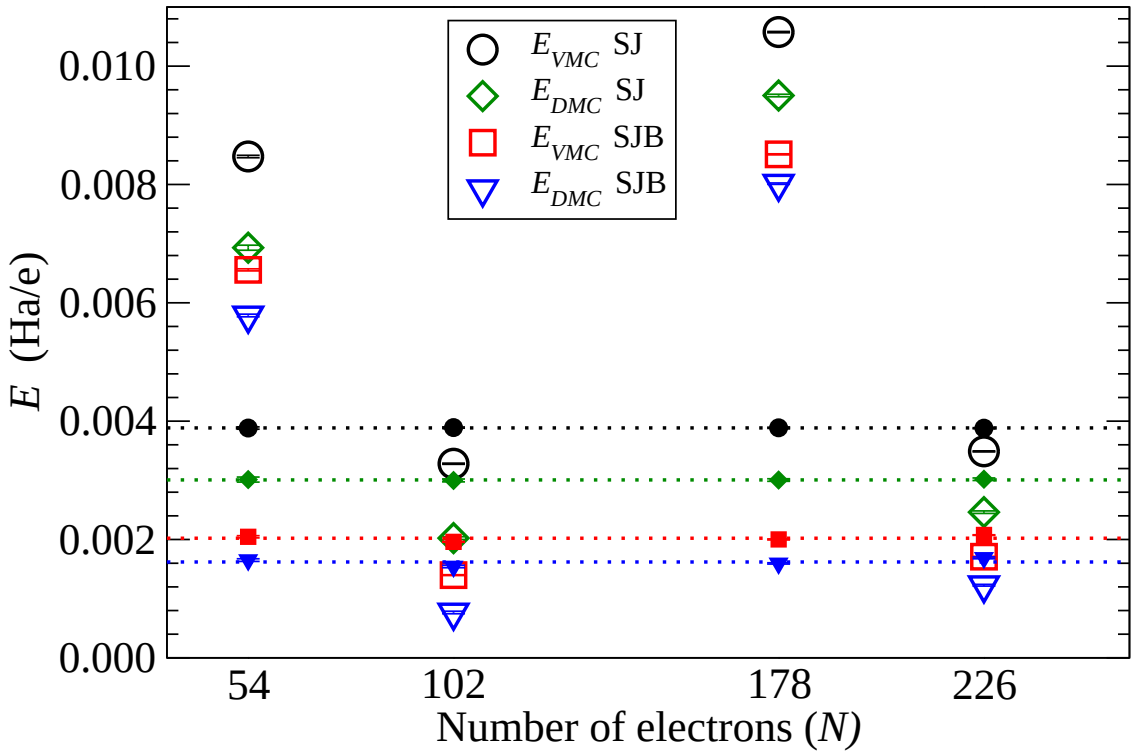


**Figure 1.** (Color online) Big open symbols: VMC and DMC ground-state total energies, $E_{VMC}$ and $E_{DMC}$, from table 1. Horizontal dotted lines: The extrapolated values $E_\infty$ (also quoted in table 1), as obtained from Equation (7). Small filled symbols: The extrapolated values, $E_N - b_1\,\Delta T_{\rm HF}(N) - \frac{b_2}{N}$, that we have obtained from Equation (7) for each $N$ and fixed values of $b_1$ and $b_2$.

The issue of finite-size corrections to the kinetic and interaction contributions to the ground-state energy has been adressed by Ceperley and co-workers [1, 37, 10, 15]. They proposed separate extrapolation terms for the kinetic and interaction contributions using the following extrapolation formula:

$$E_N = E_\infty + b_1 \, \Delta T_{\rm HF}(N) + \frac{b_2}{N}, \tag{7}$$

where $E_\infty$, $b_1$, and $b_2$ are parameters to be fitted. $\Delta T_{\rm HF}(N)$ is the difference between the Hartree-Fock kinetic energies of the finite and infinite systems, $\Delta T_{\rm HF}(N) = T_{\rm HF}(N) - T_{\rm HF}(\infty)$, and the term $b_2/N$ accounts for the finite-size effects arising in the interaction energy. Recently it has been shown that the $b_2/N$ term also corrects for the neglect of long-range correlation effects in the kinetic energy [33].

Ortiz and Ballone [14] considered an extrapolation of the form

$$E_N = E_\infty + \Delta T_{\rm HF}(N) - \left( \frac{N}{b_0} - \frac{1}{\Delta v_{\rm HF}(N)} \right)^{-1}, \tag{8}$$

with only 2 parameters to be fitted, $E_\infty$ and $b_0$. $\Delta v_{\rm HF}(N)$ in Equation (8) is the difference between the Hartree-Fock exchange energies of the finite and infinite system, $\Delta v_{\rm HF}(N) = v_{\rm HF}(N) - v_{\rm HF}(\infty)$. [+] Equation (7) and (8) were found to yield similar results. We have found, however, that Equation (7) yields in all cases better fits of the QMC data, so that all our extrapolations have been carried out by using Equation (7).[*] The horizonal dotted lines of figure 1 display the extrapolated values $E_\infty$ (also quoted in table 1) that we have found from Equation (7). These extrapolated values indicate that the optimization of the nodes of the trial wave function (which is achieved by replacing the SJ trial wave function by the SJ-backflow trial wave function) lowers the ground-state energy considerably:[♯] 2 mHa/e at the VMC level and 1.4 mHa/e at the DMC level; moreover, the optimized VMC-SJB ground-state energy happens to be 1 mHa/e lower than its fixed-node counterpart DMC-SJ.

Our extrapolated VMC and DMC ground-state total energies, $E_\infty$, are compared in table 2 and figure 2 to the corresponding energies reported in [1, 13, 14, 15]. These are: (i) the original VMC calculation of Ceperley [1], (ii) the released-node DMC calculation of Ceperley and Alder [13], (iii) the fixed-node VMC and DMC calculations of Ortiz and Ballone [14] and Kwon *et al.* [15], and (iv) the backflow DMC calculation of Kwon *et al.* [15]. We note that the DMC calculations reported by Ortiz and Ballone (OB-DMC-SJ)[14] and Kwon *et al.* (KCM-DMC-SJ and KCM-DMC-SJB) [15], were all carried out by first fitting within VMC the $E_\infty$, $b_0$, $b_1$, and $b_2$ parameters entering Equation (7) and (8) and then using the VMC parameters $b_0$, $b_1$, and $b_2$ to derive $E_\infty$ for a given $N$ from either Equation (7) or (8); hence, in order to compare to the results reported

[+] Since the exchange hole entering the Hartree-Fock exchange energy is very long ranged compared to the exchange-correlation hole, the finite-size correction $\Delta v_{\rm HF}(N)$ entering Equation (8) might not be appropriate in an extrapolation scheme for QMC energies.

[*] The adjusted R-squared values for the fits are: VMC-SJ: 0.999995, VMC-SJB: 0.999395, DMC-SJ: 0.999004, and DMC-SJB: 0.999983.

[♯] This corroborates the result reported in [16] to a small system of 54 electrons.

**Table 2.** Top: The extrapolated VMC and DMC ground-state total energies $E_\infty$ of table 1, as obtained with the use of SJ and SJB trial wave functions for a HEG of $r_s = 2$. Middle: The VMC calculation of Cerperley (C-VMC) [1], the released-node DMC calculation of Ceperley and Alder (CA-DMC-RN) [13], the fixed-node VMC and DMC calculations of Ortiz and Ballone (OB-VMC-SJ and OB-DM-SJ) [14] and Kwon *et al.* (KCM-VMC-SJ and KCM-DMC-SJ) [15], and the backflow DMC calculation of Kwon *et al.* (KCM-DMC-SJB) [15]. Bottom: DMC ground-state total energies, but now obtained by using (as in [14] and [15]) the VMC parameters $b_1$ and $b_2$ (which differ considerably from the corresponding DMC parameters) to derive $E_\infty$ for a given $N$ from Equation (7) (DMC-SJ* and DMC-SJB*).

| | $E_\infty$ (Ha/e) | Reference |
|---|---|---|
| VMC-SJ | 0.003886(5) | This work |
| VMC-SJB | 0.002021(4) | This work |
| DMC-SJ | 0.00301(1) | This work |
| DMC-SJB | 0.001621(7) | This work |
| C-VMC | 0.002955 | [1] |
| CA-DMC-RN | 0.002055 | [13] |
| OB-VMC-SJ | 0.0051(2) | [14] |
| OB-DMC-SJ | 0.0033(2) | [14] |
| KCM-VMC-SJ | 0.004096 | [15][a] |
| KCM-DMC-SJ | 0.002431 | [15][a] |
| KCM-DMC-SJB | 0.001812 | [15][a] |
| DMC-SJ* | 0.00266(1) | This work |
| DMC-SJB* | 0.001380(8) | This work |

[a] These numbers for $r_s$=2 were obtained by using an updated form of Equation (2) of [38], which was originally derived by fitting three values of $r_s$ ($r_s$= 1, 5 and 10) of [15] and we have now fitted with the four available values of $r_s$ ($r_s$= 1, 5, 10 and 20) of [15] for each case (VMC-SJ, DMC-SJ and DMC-SJB). Differences between the energies derived from Equation (2) of [38] and the numbers reported here for $r_s$=2 are within $7 \times 10^{-5}$ Ha/e.

by these authors we have performed additional DMC fits (DMC-SJ* and DMC-SJB* represented by dotted lines in figure 2) by following this approximate extrapolation procedure. With this aim, we have calculated $E_\infty$ from the DMC-SJ(B) data and the $b_1$ and $b_2$ parameters of the VMC-SJ fit for each system size $N$, and then we have fitted a horizontal line to obtain the extrapolated DMC-SJ(B)* value reported in table 2.

We find that (i) our DMC-SJ* calculation is very close to the corresponding calculation reported by Kwon *et al.* (KCM-DMC-SJ) [15], and (ii) our DMC-SJB* calculation is considerably lower than the corresponding KCM-DMC-SJB calculation, which is a signature of the better quality of our SJB trial wave functions. We note that our calculations were performed using the MPC interaction, while in the calculations reported in the above references the Ewald interaction was used. Hence, we have repeated our DMC-SJ and DMC-SJB calculations using the usual $1/r$ Ewald interaction; these calculations (shown in table 1 for DMC-SJ) indicate that in both cases the Ewald

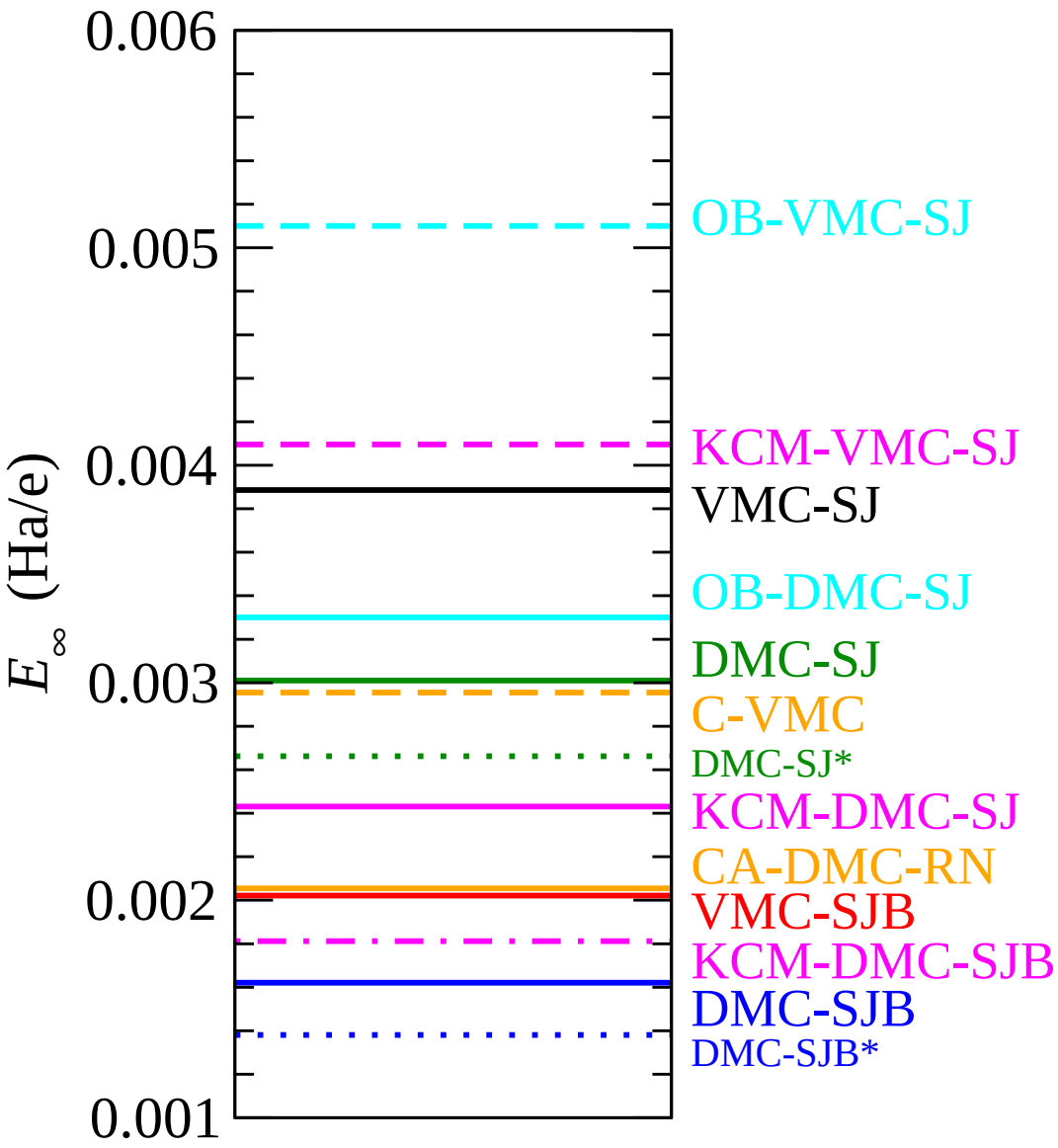


**Figure 2.** (Color online) Schematic representation of the extrapolated energies quoted in table 2.

extrapolated energy is at most 0.3 mHa/e above the MPC extrapolated result, which reflects the fact that after extrapolation to $N \to \infty$ the usual Ewald energy yields fairly good results. We note, however, that the difference between the MPC and Ewald DMC-SJ energy reported in table 1 for each N is significantly smaller than the finite-size correction proposed in [33] ($\Delta V = \omega_p/(4N)$, where $\omega_p$ is the plasmon energy). This is because the MPC and Ewald energies in table 1 were obtained using different interaction schemes in the branching part of the calculation, i. e., MPC and Ewald, respectively. We have performed additional calculations of MPC energies using the Ewald interaction in the branching factors, and we have found that only when the same interaction (Ewald) is used in the branching part of the calculation, the difference between the MPC and Ewald energies agrees with the correction proposed by Chiesa *et. al* [33].

At this point, we focus our attention on a comparison between the DMC extrapolated values that we have obtained by (i) fitting within DMC the $E_\infty$, $b_1$, and $b_2$ parameters entering Equation (7) (DMC-SJ and DMC-SJB) and (ii) using the VMC parameters $b_1$ and $b_2$ to derive $E_\infty$ for a given $N$ from Equation (7) (DMC-SJ* and DMC-SJB*). Our calculations indicate that the size-dependences for VMC and DMC differ considerably;†† indeed, the DMC-SJ* and DMC-SJB* extrapolated values are too low, i.e., the use of VMC data to extrapolate the corresponding DMC calculations yields artificially lowered extrapolations. Hence, the KCM-DMC-SJB ground-state energy reported by Kwon *et al.* [15] nearly coincides with our more accurate DMC extrapolation (DMC-SJB) as a result of two competing effects: the KCM-DMC-SJB extrapolated energy is (i) higher than our better optimized DMC-SJB* calculation and (ii) too low due to the assumption (in the extrapolation procedure) that the VMC and DMC size dependences coincide.

Finally, we note that although the fitting parameters $b_1$ and $b_2$ entering Equation (7) are not transferable from VMC to DMC calculations they are indeed transferable from DMC-SJ to the more expensive DMC-SJB calculations: The error introduced by using the DMC-SJ parameters $b_1$ and $b_2$ to derive the DMC-SJB $E_\infty$ for a given $N$ from Equation (7) is found to be of no more than 0.04(1) mHa/e.

### *4.2. Interaction energy*

The interaction energy, $\hat{U}$, is a local operator (i.e., diagonal in real space) that does not commute with the Hamiltonian. Hence, for an accurate calculation of the true expectation value of $\hat{U}$ we have applied the HF-based method of [19] described in section 2.2. Figure 3 and table 3 show the results that we have obtained for the true (HF) fixed-node interaction energies $U_{FN} = \langle \hat{U} \rangle_{HF}$ of a HEG of $r_s = 2$ for $N = 54$, 102, 178, and 226 electrons, as obtained by using either SJ or SJB trial wave functions. Also shown are the fixed-node interaction energies $U_{FN\text{–}DMC} = \langle \hat{U} \rangle_{FN\text{–}DMC}$ that we have obtained by using the standard DMC estimator, which are subject to an error that is linear in the difference between $\Psi_T$ and $\Psi_0^{FN}$.

In order to obtain the extrapolated value $U_\infty$ from our finite-size calculations, we use the fitting equation

$$U_N = U_\infty + \frac{b}{N} \tag{9}$$

for each set of data. The $1/N$ term does not aim at correcting the long-ranged errors, as we are using the MPC interaction. It turns out, however, that the residual effects including shell-filling and the distortion of the xc hole due to the finite size geometry also seem to be well described by a 1/N fit. The extrapolated values are displayed by the entry $N = \infty$ of table 3 and the solid lines of figure 3, together with the result of using

††Since the form and optimisation of the trial wave function entering VMC calculations is size-dependent, in general, there is no reason to expect VMC and DMC finite-size extrapolations to be the same.

**Table 3.** Top: The fixed-node interaction energy of a HEG with $r_s$=2 for $N$= 54, 102, 178, and 226 electrons, as obtained by using the HF-based method of [19] ($U_{FN}$) and by using the standard DMC estimator ($U_{FN-DMC}$); both SJ and SJB trial wave functions have been used. The entry $N = \infty$ corresponds to the extrapolated values obtained from Equation (9). Bottom: The extrapolated estimator $2U_{FN-DMC} - U_{VMC}$ for the infinite system. All energies are in Ha/e.

| | SJ wave function | | SJB wave function | |
|---|---|---|---|---|
| $N$ | $U_{FN}$ | $U_{FN-DMC}$ | $U_{FN}$ | $U_{FN-DMC}$ |
| 54 | -0.2993(1) | -0.29839(9) | -0.3009(1) | -0.30050(9) |
| 102 | -0.29872(8) | -0.2980(1) | -0.3005(1) | -0.2999(1) |
| 178 | -0.29782(7) | -0.29741(6) | -0.3001(1) | -0.29958(9) |
| 226 | -0.2978(1) | -0.29689(9) | -0.2996(1) | -0.2991(1) |
| $\infty$ | -0.2973(1) | -0.29679(8) | -0.2994(1) | -0.2990(1) |

| | $2U_{DMC} - U_{VMC}$ (Ha/e) |
|---|---|
| SJ ($N = \infty$) | -0.29764(8) |
| SJB($N = \infty$) | -0.2997(1) |

**Table 4.** The fixed-node extrapolated interaction energy ($U_\infty$) for each system size as obtained from the fits of Equation (9) of the interaction energies of table 3.

| | SJ wave function | | SJB wave function | |
|---|---|---|---|---|
| $N$ | $U_{FN}$ | $U_{FN-DMC}$ | $U_{FN}$ | $U_{FN-DMC}$ |
| 54 | -0.2970(2) | -0.2967(2) | -0.2993(2) | -0.2990(2) |
| 102 | -0.2975(1) | -0.2971(1) | -0.2997(1) | -0.2991(1) |
| 178 | -0.29714(9) | -0.29689(7) | -0.2996(1) | -0.2991(1) |
| 226 | -0.2973(1) | -0.29648(9) | -0.2992(1) | -0.2988(1) |

the extrapolated estimator $2U_{FN-DMC} - U_{VMC}$ for the infinite system (dotted and dashed-dotted lines). We see that while the true interaction energy $U_{FN}$ is overestimated by the standard DMC estimator $U_{FN-DMC}$ (the error being linear in the difference between $\Psi_T$ and $\Psi_0^{FN}$), it is underestimated by the extrapolated estimator $2U_{FN-DMC} - U_{VMC}$ (the error this time being quadratic in the difference between $\Psi_T$ and $\Psi_0^{FN}$). On the other hand, we see that as in the case of the ground-state total energy the effect of backflow (included in the calculations labeled SJB) is to lower the interaction energy by a rigid shift of about 2 mHa/$e$. Finally, we note that error bars in figure 3 are approximately the size of the symbols (about 0.1 mHa/e), even for the largest systems under consideration. Table 4 summarizes the extrapolated values for each system size, $U_\infty = U_N - b/N$, for all the cases shown in table 3.

In a recent paper [39], it was demonstrated that accurate calculations of the interaction contribution to the ground-state energy of an arbitrary many-electron system can be obtained from the knowledge of the spherically averaged wavevector-dependent

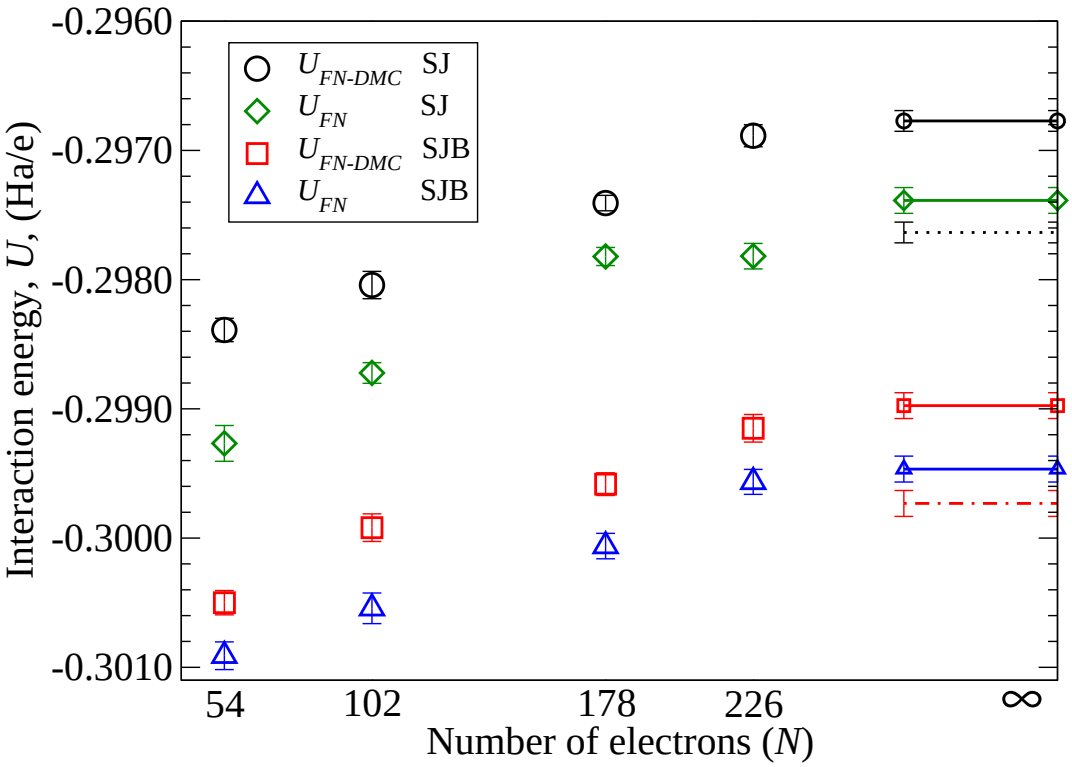


**Figure 3.** (Color online) Open symbols: The fixed-node interaction energies $U_{FN}$ and $U_{FN-DMC}$ quoted in table 3. Open symbols joined by solid horizontal lines: The extrapolated interaction energies obtained from Equation (9). Black dotted and red dashed-dotted lines: The extrapolated estimator $2U_{FN-DMC} - U_{VMC}$ for the infinite system, as obtained with the use of SJ (black dotted line) and SJB (red dashed-dotted line) trial wave functions.

diagonal structure factor $S_k$ as follows

$$U = \frac{1}{\pi} \int [S_k - 1] \, \mathrm{d}k, \tag{10}$$

where $S_k$ is the spherical average of the diagonal structure factor in Fourier space:

$$S_k = 1 + \frac{4\pi}{N} \int \mathrm{d}\mathbf{r} n(\mathbf{r}) \int \mathrm{d}u \, u^2 \frac{\sin(ku)}{ku} n_{xc}(\mathbf{r}, u). \tag{11}$$

Here, $N$ is the particle number, $n(\mathbf{r})$ is the electron density at $\mathbf{r}$, and $n_{xc}(\mathbf{r}, u)$ is the spherically averaged exchange-correlation hole density $n_{xc}(\mathbf{r}, \mathbf{r}')$ at $\mathbf{r}'$ around an electron at $\mathbf{r}$. If one samples the structure factor using only correlations within the simulation cell, then Equation (10) represents the $k$-resolved MPC interaction [20].

The structure factor can be computed using VMC [39], standard DMC, or the HF-based DMC [20]. Since the spherically averaged structure factor is a diagonal function in real space, HF-based DMC calculations should yield the exact fixed-node $S_k$. Figure 4 exhibits VMC, standard-DMC (FN-DMC) and HF-based DMC (FN) calculations of $S_k$ for a HEG with $r_s = 2$ and $N$=102 electrons, as obtained with the use of SJ wave functions. Equation (10) then yields the following VMC, standard-DMC, and HF-based DMC interaction energies: -0.29717(3) Ha/e, -0.2979(1) Ha/e,

and -0.29871(8) Ha/e, respectively, which agree with our calculated expectation values $\langle\hat{U}\rangle_{VMC} = -0.29719(3)$ Ha/e, $\langle\hat{U}\rangle_{FN-DMC} = -0.2980(1)$ Ha/e, and $\langle\hat{U}\rangle_{HF} = -0.29872(8)$ Ha/e (see also table 3), as expected.

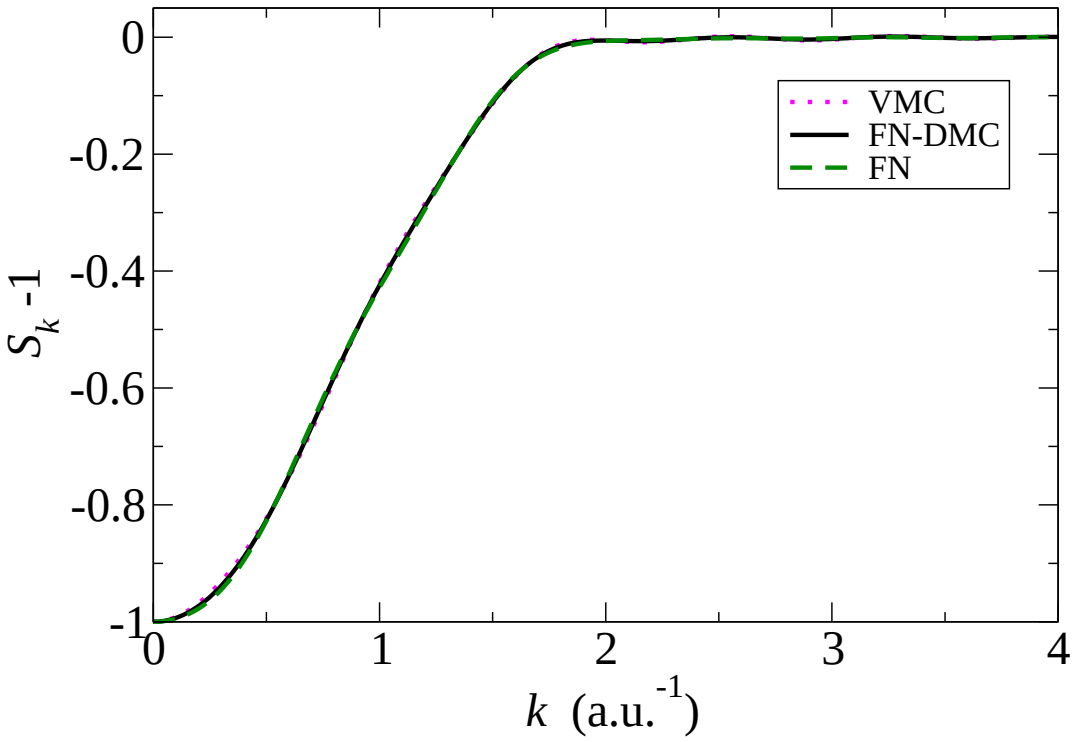


**Figure 4.** (Color online) VMC, standard-DMC, and HF-based DMC calculations of the spherically averaged structure factor $S_k$ of a HEG with $r_s$=2 and $N$=102 electrons, as obtained with the use of SJ trial wave functions.

### *4.3. Kinetic energy*

**Table 5.** Standard-DMC (top) and HF-based DMC (bottom) kinetic and interaction energies, as obtained in the thermodinamic limit ($N \to \infty$) with the use of SJ and SJB wave functions. $\Delta = |SJ - SJB|$ denotes the absolute value of the difference between the SJ and SJB calculations.

| | $U_\infty$ (Ha/e) | T$_\infty$(Ha/e) |
|---|---|---|
| FN-DMC SJ | -0.29679(8) | 0.29980(8) |
| FN-DMC SJB | -0.2990(1) | 0.3006(1) |
| $\Delta$=\|SJ-SJB\| | $22(1)10^{-4}$ | $8(1)10^{-4}$ |
| FN SJ | -0.2973(1) | 0.3003(1) |
| FN SJB | -0.2994(1) | 0.3011(1) |
| $\Delta$=\|SJ-SJB\| | $22(1)10^{-4}$ | $8(1)10^{-4}$ |

Assuming that the ground-state interaction and total energies have been correctly extrapolated, the kinetic energy can be obtained in the thermodynamic limit as

$T_\infty = E_\infty - U_\infty$. Table 5 shows standard-DMC and the more accurate HF-based DMC calculations of $T_\infty$, as obtained from the corresponding standard-DMC and HF-based DMC calculations of $U_\infty$ (also quoted) with the use of either SJ or SJB trial wave functions. The absolute value of the difference between the SJ and SJB calculations ($\Delta = |\mathrm{SJ} - \mathrm{SJB}|$) is also shown in this table. We note that this difference is considerably larger for the interaction energy, both in the case of the standard DMC approach and in the case of the more accurate HF-based DMC approach. This is an indication of the fixed-node error being smaller in the kinetic energy than in the interaction energy. Indeed, the correlation contribution to the kinetic energy is always smaller than the corresponding contribution to the interaction energy.

## 5. Conclusions

We have presented benchmark VMC and DMC ground-state energies of a 3D HEG with $r_s = 2$ and $N$=54, 102, 178, and 226 electrons, using an MPC interaction and backflow corrections. We have extrapolated our finite-size calculations to the thermodynamic limit, and we have found lower energies than previously reported, thus showing the good quality of our fixed-node trial wave functions. We have shown that previously extrapolated results are artificially lowered by assuming that the VMC and DMC size dependences (which we analyze independently) coincide. We have used the HF operator sampling method introduced in [19] to compute accurate values of the kinetic and interaction contributions to the ground-state energy. We also show that these values, as obtained with the use of the MPC interaction, coincide with the result one obtains from the spherically averaged structure factor. Our calculations indicate that our HF-based DMC approach yields very accurate results even for very large systems. Finally, we have found that the difference between the interaction energies that we obtain using either the original Slater-determinant nodes or the backflow-displaced nodes is considerably larger than the difference between the corresponding kinetic energies. A combination of (i) the fact that our Hellman-Feynman operator sampling method allows, within the fixed-node approximation, to calculate accurately the kinetic-energy contribution to the ground-state energy and (ii) the fact that the fixed-node error is smaller in the kinetic energy than in the interaction and total ground-state energy leads us to the conclusion that our kinetic energies should be of great use in the construction of accurate kinetic-energy functionals.

## Acknowledgments

This work was partially supported by the Basque Government (Grant No. GIC07IT36607) and the Spanish Ministerio de Educación y Ciencia (Grant. No. FIS2006-01343 and CSD2006-53). Computing facilities were provided by the Donostia International Physics Center (DIPC) and the SGI/IZO-SGIker UPV/EHU (supported by the National Program for the Promotion of Human Resources within the National

Plan of Scientific Research, Development and Innovation-Fondo Social Europeo, MCyT and the Basque Government).

## References

[1] D. M. Ceperley. Ground state of the fermion one-component plasma: A Monte Carlo study in two and three dimensions. *Phys. Rev. B*, 18:3126, 1978.

[2] W. M. C. Foulkes, L. Mitaš, R. J. Needs, and G. Rajagopal. Quantum Monte Carlo simulations of solids. *Rev. Mod. Phys.*, 73:33, 2001.

[3] James B. Anderson. Quantum chemistry by random walk. H $^2$P, $H_3^+$ $D_3h$ $^1$A'$_1$, $H_2$ $^3\Sigma_u^+$, $H_4$ $^1\Sigma_g^+$, Be $^1$S. *J. Chem. Phys.*, 65:4121, 1976.

[4] A. Ma, N. D. Drummond, M. D. Towler, and R. J. Needs. All-electron quantum Monte Carlo calculations for the noble gas atoms He to Xe. *Phys. Rev. E*, 71:066704, 2005.

[5] N. D. Drummond, P. López Ríos, A. Ma, J. R. Trail, G. G. Spink, M. D. Towler, and R. J. Needs. Quantum Monte Carlo study of the Ne atom and the Ne+ ion. *J. Chem. Phys.*, 124:224104, 2006.

[6] I. G. Gurtubay, N. D. Drummond, M. D. Towler, and R. J. Needs. Quantum Monte Carlo calculations of the dissociation energies of three-electron hemibonded radical cationic dimers. *J. Chem. Phys.*, 124:024318, 2006.

[7] I. G. Gurtubay and R. J. Needs. Dissociation energy of the water dimer from quantum Monte Carlo calculations. *J. Chem. Phys.*, 127:124306, 2007.

[8] Ryo Maezono, A. Ma, M. D. Towler, and R. J. Needs. Equation of state and Raman frequency of diamond from quantum Monte Carlo simulations. *Phys. Rev. Lett.*, 98:025701, 2007.

[9] E. Sola, J. P. Brodholt, and D. Alfè. Equation of state of hexagonal closed packed iron under earths core conditions from quantum Monte Carlo calculations. *Phys. Rev. B*, 79:024107, 2009.

[10] B. Tanatar and D. M. Ceperley. Ground state of the two-dimensional electron gas. *Phys. Rev. B*, 39:5005, 1989.

[11] Claudio Attaccalite, Saverio Moroni, Paola Gori-Giorgi, and Giovanni B. Bachelet. Correlation energy and spin polarization in the 2D electron gas. *Phys. Rev. Lett*, 88:256601, 2002.

[12] N. D. Drummond and R. J. Needs. Quantum Monte Carlo study of the ground state of the two-dimensional fermi fluid. *Phys. Rev. B*, 79(085414), 2009.

[13] D. M. Ceperley and B. J. Alder. Ground state of the electron gas by a stochastic method. *Phys. Rev. Lett.*, 45:566, 1980.

[14] G. Ortiz and P. Ballone. Correlation energy, structure factor, radial distribution function, and momentum distribution of the spin-polarized uniform electron gas. *Phys. Rev. B*, 50:1391, 1994.

[15] Yongkyung Kwon, D. M. Ceperley, and Richard M. Martin. Effects of backflow correlation in the three-dimensional electron gas: Quantum Monte Carlo study. *PRB*, 58:6800, 1998.

[16] P. López Ríos, A. Ma, N. D. Drummond, M. D. Towler, and R. J. Needs. Inhomogeneous backflow transformations in quantum Monte Carlo. *Phys. Rev. E*, 74:066701, 2006.

[17] F. H. Zong, C. Lin, and D. M. Ceperley. Spin polarization of the low-density three-dimensional electron gas. *Phys. Rev. E*, 66:036703, 2002.

[18] M. Holzmann, D. M. Ceperley, C. Pierleoni, and K. Esler. Backflow correlations for the electron gas and metallic hydrogen. *Phys. Rev. E*, 68:046707, 2003.

[19] R. Gaudoin and J. M. Pitarke. Hellman-Feynman operator sampling in diffusion Monte Carlo calculations. *Phys. Rev. Lett.*, 99:126406, 2007.

[20] R. Gaudoin, I. G. Gurtubay, and J. M. Pitarke. To be published.

[21] R. J. Needs, M. D. Towler, N .D Drummond, and P. López Ríos. CASINO *version 2.1.400 User Manual*. University of Cambridge, Cambridge, 2007.

[22] N. D. Drummond, M. D. Towler, and R. J. Needs. Jastrow correlation factor for atoms, molecules, and solids. *Phys. Rev. B*, 70:235119, 2004.

[23] M. H. Kalos. Stochastic wave function for atomic helium. *J. Comput. Phys.*, 1:257, 1966.

[24] N. R. Barnett, P. J. Reynolds, and W. A. Lester. Monte Carlo algorithms for expectation values of coordinate operators. *J. Comput. Phys.*, 96:258, 1991.

[25] Stefano Baroni and Saverio Moroni. Reptation quantum Monte Carlo: A method for unbiased ground-state averages and imaginary-time correlations. *Phys. Rev. Lett.*, 82:4745, 1999.

[26] Roland Assaraf and Michel Caffarel. Zero-variance zero-bias principle for observables in quantum Monte Carlo: Application to forces. *J. Chem. Phys.*, 119:10536, 2003.

[27] R. Gaudoin and J. M. Pitarke. To be published.

[28] P. R. C. Kent, R. J. Needs, and G. Rajagopal. Monte Carlo energy and variance-minimization techniques for optimizing many-body wave functions. *Phys. Rev. B*, 59:12344, 1999.

[29] N. D. Drummond and R. J. Needs. Variance-minimization scheme for optimizing Jastrow factors. *Phys. Rev. B*, 72:085124, 2005.

[30] M. D. Brown. *Energy Minimisation in Variational Quantum Monte Carlo*. PhD thesis, University of Cambridge, 2007.

[31] N. D. Drummond, R. J. Needs, A. Sorouri, and W. M. C. Foulkes. Finite-size errors in continuum quantum Monte Carlo calculations. *Phys. Rev. B*, 78:125106, 2008.

[32] C. Lin, F. H. Zong, and D. M. Ceperley. Twist-averaged boundary conditions in continuum quantum Monte Carlo algorithms. *Phys. Rev. E*, 64:016702, 2001.

[33] Simone Chiesa, David M. Ceperley, Richard M. Martin, and Markus Holzmann. Finite-size error in many-body simulations with long-range interactions. *Phys. Rev. Lett.*, 97:076404, 2006.

[34] Louisa M. Fraser, W. M. C. Foulkes, G. Rajagopal, R. J. Needs, S. D. Kenny, and A. J. Williamson. Finite-size effects and coulomb interactions in quantum Monte Carlo calculations for homogeneous systems with periodic boundary conditions. *Phys. Rev. B*, 53, 1996.

[35] A. J. Williamson, G. Rajagopal, R. J. Needs, L. M. Fraser, W. M. C. Foulkes, Y. Wang, and M.-Y. Chou. Elimination of coulomb finite-size effects in quantum many-body simulations. *Phys. Rev. B*, 55:R4851, 1997.

[36] P. R. C. Kent, Randolph Q. Hood, A. J. Williamson, R. J. Needs, W. M. C. Foulkes, and G. Rajagopal. Finite-size errors in quantum many-body simulations of extended systems. *Phys. Rev. B*, 59:1917, 1999.

[37] D. M. Ceperley and B. J. Alder. Ground state of solid hydrogen at high pressures. *Phys. Rev. B*, 36:2092, 1987.

[38] J. M. Pitarke. Comment on Diffusion Monte Carlo study of jellium surfaces: Electronic densities and pair correlation functions. *Phys. Rev. B*, 70:087401, 2004.

[39] R. Gaudoin and J. M. Pitarke. Quantum Monte Carlo modelling of the spherically averaged structure factor of a many-electron system. *Phys. Rev. B*, 75:155105, 2007.